

# The Question of Solid-State Electron Transfer in Contact Charging between Metal and Organic Materials

J. Guay, J. E. Ayala, and A. F. Diaz\*

IBM Almaden Research Center K41/803, 650 Harry Road, San Jose, California 95120

Le H. Dao

INRS Energie, 1650 Montee Sainte-Julie, Varennes, Quebec J3X 1S2, Canada

Received June 17, 1991. Revised Manuscript Received August 20, 1991

This report describes charging studies between iron beads and powders of some aromatic anil derivatives that were previously used to study the mechanism of charging. Our results show that the charge responses to substituent effects and linear correlations are observed between the charge and both the oxidation potentials and the basicity of the compounds. These parallel relationships question the validity of previous conclusions proposing electron transfer as the basis for charging. We also find that the charging is accompanied by a considerable amount of material transfer to the iron beads, which points to the inadequacy of selecting these materials for mechanistic studies. The need to invoke electron transfer to explain the charge is questioned based on the relative energetics of the proton- and electron-transfer process.

## Introduction

Contact electrification, or triboelectrification, is the charge buildup on the surfaces of two dissimilar materials (solids) when they are contacted (with or without friction) and separated. The current interest in surface charging with organic and with ceramic materials lies in its importance in electrophotography<sup>1,2</sup> and its damaging effects on electronic components.<sup>3,4</sup> Although contact charging has been studied for many years,<sup>5-7</sup> the origin of charge exchange with insulating materials remains controversial and has been attributed to both ionic<sup>8,9</sup> and electron transfer.<sup>10,11</sup> Some years ago, Cressman et al.<sup>12</sup> and Gibson<sup>13</sup> studied the solid-state charge transfer between a metal and two well-defined series of substituted aromatic compounds. In one of these experiments,<sup>12</sup> charge was developed by rolling spherical nickel beads (250- $\mu$ m diameter) down an inclined plane coated with a film of various 1-(para-substituted phenylazo)-2-naphthols (X-Ph-azo-Np) derivatives. A linear relationship was obtained between the charge and the Hammett substituent constant ( $\sigma$ ), even though some compounds charged positive and some negative. The existence of this relationship led the authors to propose a solid-state electron-transfer mechanism for charging. One year later Gibson<sup>13</sup> reported a similar study using a series of substituted salicylaldehyde anils and substituted polystyrenes. The charging was again developed by rolling spherical stainless steel beads (250- $\mu$ m diameter) down an inclined plane coated with a film of organic material. The anil derivatives charged more positive than those in Cressman's study, and none of them charged negative. However, in contrast with Cressman's results, it was the log of the charge that was linear with the Hammett  $\sigma$  constant. Electron transfer was again invoked to explain these results; however, the log-linear discrepancy in the relationship with  $\sigma$  between the two

studies was not resolved or even discussed. The electron transfer is believed to occur from the donating energy levels (HOMO) of the organic compounds, e.g., the phenylazonaphthols or the aromatic anil derivatives, to the Fermi level of the metal when the organic materials are positively charged and from the Fermi level of the metal to the accepting energy levels (LUMO) of the organic derivatives when the latter charge negative (Figure 1). In fact, Gibson described this process as solid-state electrochemistry by analogy with the electron-exchange process proposed for contact charging with metals.<sup>14</sup>

There are two major concerns with the proposed electron-transfer mechanism.<sup>12,13</sup> First, linear relationships between charge and the Hammett  $\sigma$  constant are not sufficient to distinguish between an electron-exchange and a proton-exchange process because the same qualitative trends are produced by both. It should be kept in mind that the Hammett constant is based on the proton dissociation reaction of benzoic acid.<sup>15</sup> Second, the change in the sign of the charge with the X-Ph-azo-Np derivatives (positive with the dimethylamino and methoxy substituents, and negative with the methyl, chloro, hydrogen, and nitro substituents) indicates a change in the transfer direction of electron or ion transfer. To comply with the electron-transfer mechanism, the HOMO energy level of the compounds that charge positive and LUMO energy levels of the compounds that charge negative are both required to be close to the Fermi level of the metal as shown schematically in Figure 1. Thus the change in the sign of the charge requires the energy of the molecular orbitals of these compounds to shift by ca. 2.4 eV along the series; this value is from the oxidation and reduction potentials for this class of compounds.<sup>12</sup> Not only is this unrealistic, but the range in the oxidation potentials within the series suggests a maximum shift of less than 0.8 eV. More recently, the same charge-structure correlations were used with a series of ionomers containing substituted arylphosphonium arylsulfonate salts.<sup>2,16</sup> Observation of the linear relationship between log (charge) and  $\sigma$  led the authors to again propose the electron-transfer mechanism.

Ion transfer was recently proposed to explain the charging behavior of polymers containing minor amounts of molecular salts and ionomers when contacted by a

(1) Dessauer, J. H.; Clark, A. E. *Xerography and Related Processes*; Focal Press: New York, 1965.

(2) Anderson, J. H.; Bugner, D. E. U.S. Patent 4,837,391, 1989.

(3) Davis, D. K. *J. Electrostat.* 1985, 16, 329.

(4) Crockett, R. G. M.; Hughes, J. F.; Pude, J. R. G.; Sing, H. M. *J. Electrostat.* 1985, 16, 343.

(5) *Encyclopedia Britannica*; Chicago, IL, 1955; Vol 8, p 169.

(6) Gilbert, W. *De Magnete*; London, 1600.

(7) Lichtenberg, G. C. *Novi Comment. Gottingen* 1777, 8, 168.

(8) Kornfeld, M. I. *J. Phys. D, Appl. Phys.* 1976, 9, 1445.

(9) Henry, P. S. H. *Br. J. Appl. Phys.* 1957, 4, Suppl. 2, S6.

(10) Lowell, J. J. *J. Phys. D, Appl. Phys.* 1979, 12, 1541.

(11) Hersh, S. P.; Montgomery, D. J. *Text. Res. J.* 1956, 26, 95.

(12) Cressman, P. J.; Hartmann, G. C.; Kuder, J. E.; Saevee, F. D.; Wychick, D. J. *Chem. Phys.* 1974, 61, 2740.

(13) Gibson, H. W. *J. Am. Chem. Soc.* 1975, 97, 3832.

(14) Harper, H. R. *Proc. R. Soc. London, A* 1951, 205, 83.

(15) Stock L. M.; Brown H. C. In *Advances in Physical Organic Chemistry*; Academic Press: New York, 1963; p 35.

(16) Bugner, D. E.; Anderson J. H. *Polym. Prepr. (Am. Chem. Soc., Div. Polym. Chem.)* 1988, 29, 643.

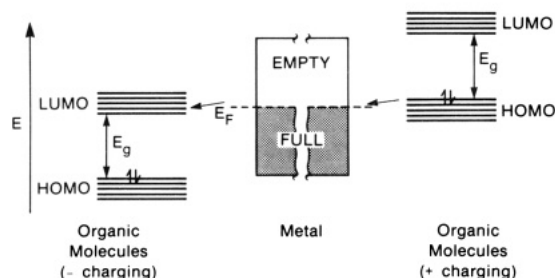
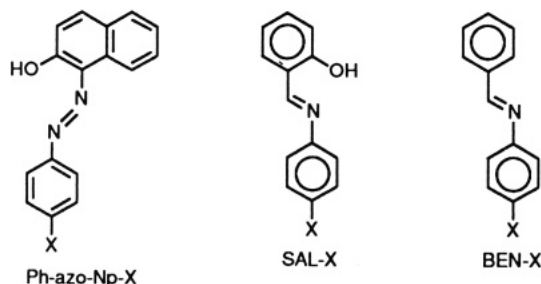


**Figure 1.** Energy schematic for metal and polymer for a positive and negative charging polymer. Note that the energy levels ( $E_F$ , LUMO, and HOMO) of the metal and the organic compounds do not need to be energetically matched for electron transfer to occur if there is band bending.

metal.<sup>17,18</sup> In these studies, the conclusion is based on the direct observation of the transferred ion (from the polymer) on the surface of the second material and the correlation in the sign of the ion and the contact charge. In one study an ionomer composed of styrene and *N*-methylvinylpyridinium toluenesulfonate in a styrene-butyl methacrylate copolymer host was used. On contact, this material developed a positive charge and the second surface a negative charge. XPS analysis of the second surface after contact showed the presence of sulfur for the toluenesulfonate.<sup>17</sup> In another study using cetylpyridinium bromide in a host polymer, the second surface developed a negative charge and SIMS analysis of the second surface after contact again revealed the presence of bromide.<sup>18</sup> In light of these results and the concerns about electron transfer mentioned above, we decided to reinvestigate the contact electrification behavior of benzaldehyde anil (BEN-X) and salicylaldehyde anil (SAL-X) derivatives and some aniline derivatives (AN-X) with metal beads.



## Experimental Section

**Materials.** The aniline derivatives (AN-X),  $\geq 99\%$  (Aldrich Chemical Co.), ferrocene (Aldrich Chemical Co.),  $\text{Bu}_4\text{NBF}_4$  (Southwestern Analytical Chemicals, Inc.), and HPLC grade acetonitrile (EM Industries, Inc.) were used as received. Salicylaldehyde anils (SAL-X) and benzaldehyde anils (BEN-X) were synthesized by the condensation of equimolar amounts of salicylaldehyde and benzaldehyde respectively with the appropriate aniline derivative by refluxing in methanol for 2 h. The crude products were then precipitated by cooling. Benzaldehyde anil was recrystallized from low-boiling petroleum ether. *p*-Methoxybenzaldehyde and salicylaldehyde anils were purified by further recrystallization from methanol.

BEN-H: mp 51.5–52.2 °C (reported<sup>19</sup> 53 °C). Anal. Calcd for  $\text{C}_{13}\text{H}_{11}\text{N}$ : C, 86.19; H, 6.07; N, 7.73. Found: C, 85.56; H, 6.17; N, 7.65.

BEN- $\text{OCH}_3$ : mp 71.6–72.1 °C. Anal. Calcd for  $\text{C}_{14}\text{H}_{13}\text{N}$ : C, 79.62; H, 6.16; N, 6.64. Found: C, 78.78; H, 6.10; N, 6.51.

(17) Diaz, A. F.; Fenzel-Alexander, D.; Miller, D. C.; Wollmann, D.; Eisenberg, A. *J. Polym. Sci. Part C: Polym. Lett.* **1990**, *28*, 75.

(18) Mizes, H. A.; Conwell, E. M.; Salameda, D. P. *Appl. Phys. Lett.* **1990**, *56*, 1597.

(19) Heilbronner, E.; Murell, J. N.; Gerson, F.; Schulze, J. *Helv. Chim. Acta* **1961**, *44*, 428.

**Table I: UV-Visible Absorption and  $E_{1/2}$  (Oxidation) Data**

derivative	$\lambda_{\text{max}}$ (log $\epsilon$ )	$E_{1/2}$ , V (vs SCE)	
<i>p</i> -X-salicylaldehyde anils			
H	338 (4.10)	1.23	1.23 <sup>a</sup>
$\text{CH}_3\text{O}$	348 (4.39)	1.14	1.15 <sup>a</sup>
<i>p</i> -X-benzaldehyde anils			
H	264 (4.25)	1.58	1.58 <sup>a</sup>
$\text{CH}_3\text{O}$	332 (4.13)	1.26	1.28 <sup>b</sup>
<i>p</i> -X-anilines			
$\text{NO}_2$	364 (4.27)	1.34	1.31 <sup>c</sup>
$\text{CH}_3$	242 (3.98)	0.79	0.78 <sup>c</sup>
$\text{CH}_3\text{O}$	242 (4.00)	0.60	0.60 <sup>c</sup>
$\text{NH}_2$	252 (3.97)	0.26	0.24 <sup>c</sup>

<sup>a</sup> Reference 33. <sup>b</sup> Reference 34. <sup>c</sup> Reference 35.

SAL-H: mp 49.8–50.8 °C (reported<sup>20</sup> 49–50 °C). Anal. Calcd for  $\text{C}_{13}\text{H}_{11}\text{N}$ : C, 79.19; H, 5.58; N, 7.11. Found: C, 79.01; H, 5.62; N, 7.07.

SAL- $\text{OCH}_3$ : mp 83.7–84.5 °C (reported<sup>20</sup> 83–84 °C). Anal. Calcd for  $\text{C}_{14}\text{H}_{13}\text{N}$ : C, 74.00; H, 5.73; N, 6.17. Found: C, 73.71; H, 5.81; N, 6.09.

**Electrochemistry.** All electrochemical measurements were made using a platinum ultramicroelectrode (Cypress Systems, Inc.) with a 5- $\mu\text{m}$  radius working electrode, a gold wire (diameter 1 mm) spiral auxiliary electrode, and a saturated calomel reference electrode in a one-compartment cell. The potential at the ultramicroelectrode was applied for a cyclic voltammetry with potentiostat/galvanostat (EG&G Model 362) and displayed directly on an X-Y recorder. All the experiments were carried out in a Faraday cage at a sweep rate of 10 mV/s. The electrolyte was a 0.1 M  $\text{Bu}_4\text{NBF}_4$  solution containing  $10^{-3}$ – $10^{-4}$  M electroactive materials. Under these conditions, ferrocene gave  $E_{1/2} = 0.40$  V and  $E_{3/4} - E_{1/4} = 60$  mV (value expected for a reversible system.).

**Charge Measurements.** The contact charge measurements were made on powders using the total blowoff technique.<sup>21</sup> The various aniline and aromatic anil derivatives were manually ground and size classified to 38–68- $\mu\text{m}$  particles by sieving. The powder (0.125 g) was then mixed with 5 g of 140- $\mu\text{m}$ -diameter irregularly shaped iron beads, and the mixture was gently rolled in a jar to activate the charge. The mixture was rolled for 3 min, which is sufficient time to equilibrate the charge. The charge remained stable up to 30 min rolling time and could be reproduced within 10%, even after several week intervals. A 1-g aliquot of the mixture was then transferred to a Faraday cage, and the organic particles were blown away from the iron beads with air (during 2 min at 56 psi) through a wire screen with 74- $\mu\text{m}$  openings. The iron beads were then recovered for further analysis. The charge/weight ratios ( $Q/M$ ) of the organic materials were measured from the total charge measured across the screen using a Keithley electrometer (Model 616) and the weight difference of the cage with the mixture before and after the blowoff experiment. The corresponding  $Q/M$  values for the beads were then calculated using the bead/powder weight ratio in the initial mixture. The measured charge was in the range 1–200 nC. The  $Q/M$  values are the average of repeat experiments with several measurements each.

**Determination of Mass Transfer.** The amount of residual organic materials remaining on the iron beads after the blowoff step was determined by UV-visible spectroscopy. For this measurements, 0.2 g of iron beads was added to 10 mL of acetonitrile, and the mixture was sonicated for 1 min. UV-visible spectra of the supernatant were measured with a diode array spectrophotometer (HP 8452A). The weight of the organic compounds in solution was calculated from the absorption maxima and using the Beer-Lambert law and then normalized to the weight of metal particles used. The molar absorption of each compound was previously determined. The absorbance values were corrected for the small background absorption inherent of beads not contacted with any compound. The values are the average of several experiments. The wavelength corresponding to the absorption maxima ( $\lambda_{\text{max}}$ ) and the logarithm of the molar absorptivity (log  $\epsilon$ ) for each compound are reported in Table I.

(20) Gooden, W. W. *Aust. J. Chem.* **1965**, *18*, 637.

(21) Schein, L. B.; Cranch, J. *J. Appl. Phys.* **1975**, *46*, 5140.

Table II: Charging and Material Transfer Data

derivative	iron beads		organic powders	
	$Q/M$ , nC/g	$N_R$ , $\mu\text{mol/g}$	$Q/M$ , $\mu\text{C/g}$	$Q/N$ , $\mu\text{C/mol}$
<i>p</i> -X-salicylaldehyde anils				
H	-55	1.7	2.2	433
CH <sub>3</sub> O	-210	2.3	8.4	1900
<i>p</i> -X-benzaldehyde anils				
H	-6.7	0.9	0.27	49
CH <sub>3</sub> O	-63	1.4	2.51	530
<i>p</i> -X-anilines				
NO <sub>2</sub>	+20	0.8	-0.8	-110
CH <sub>3</sub>	-1.0	0.4	0.04	4.3
CH <sub>3</sub> O	-7.8	1.1	0.31	38
NH <sub>2</sub>	-87	2.0	3.47	375

Scanning electron micrographs were taken on gold-sputtered samples using a Hitachi F-800 microscope. An accelerating voltage of 10 kV was used.

### Results and Discussion

Powders with 38–68- $\mu\text{m}$  diameter particles of the aniline (AN-X), benzaldehyde anil (BEN-X), and salicylaldehyde anil (SAL-X) were charged against irregularly shaped metal beads with 140- $\mu\text{m}$  diameter. The charge was activated by gently rolling a powder/bead mixture (2.5/97.5 wt %) for 3 min. The developed charge was measured by total blowoff and is expressed as the charge-to-mass ( $Q/M$ ) ratio for both the organic compounds and the iron beads. As seen in Table II, all the compounds charge positive and give the beads a negative charge except *p*-nitroaniline. The substituent effect is the same for the three derivative series where higher charge levels are generated with the presence of the electron-rich methoxy group. The charges on the iron beads after rolling with the SAL-H anil and SAL-OCH<sub>3</sub> anil powders are -55 and -210 nC/g, respectively. The corresponding surface charge densities calculated using the specific surface area (400 cm<sup>2</sup>/g<sup>22</sup>) are (1.4–5.3)  $\times 10^{-10}$  C/cm<sup>2</sup>. This corresponds to (1–3)  $\times 10^9$  negative ions/cm<sup>2</sup>, which is much lower than a monolayer coverage,  $4 \times 10^{14}$  ions/cm<sup>2</sup>, estimated for a 25 Å<sup>2</sup> footprint. The charge developed with the benzaldehyde anil and the aniline derivatives were parallel but lower. Also listed in Table II are the charge values for the organic powders expressed as charge-to-mole ratios ( $Q/N$ ). The corresponding surface charge densities of the organic particles are in the range (3–70)  $\times 10^{-10}$  C/cm<sup>2</sup> and were calculated using the surface/mass ratio ( $S/M = 3/r\rho$ ) for the particles with a median radius ( $r$ ) of 25  $\mu\text{m}$ , a density ( $\rho$ ) of 1 g/cm<sup>3</sup> and assuming a spherical geometry. The surface charge densities are typical for organic insulators when contacted with a metal in air.<sup>23</sup>

Two of the compounds, SAL-H and SAL-OCH<sub>3</sub>, were selected for this study because they were studied by Gibson,<sup>13</sup> and it permits us to calibrate the results from the two laboratories. It is not our intent to confirm Gibson's complete study; therefore, only two compounds were evaluated instead of the complete set of derivatives. The sign and trend in the charge with SAL-H and SAL-OCH<sub>3</sub> agree well with the report by Gibson;<sup>13</sup> for example, the iron beads develop a negative charge and the charge is higher with the methoxy derivative. The values reported by Gibson for these two derivatives are -0.8 and -1.5 nC/g,<sup>13</sup> which corresponds to (0.27–0.5)  $\times 10^{-10}$  C/cm<sup>2</sup>. The latter were estimated using a density of 7.9 g/cm<sup>3</sup> and a

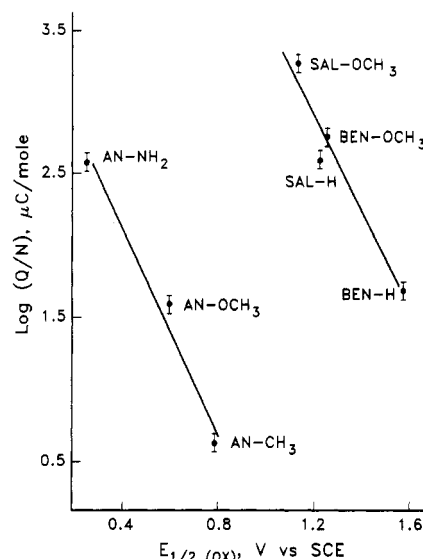
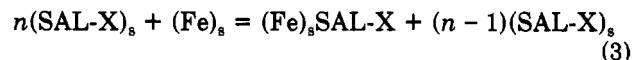
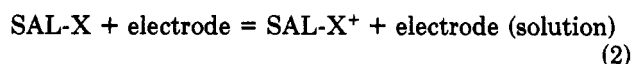


Figure 2. Plot of  $\log (Q/N)$  against  $E_{1/2}$  (vs SCE) for the substituted aniline, benzaldehyde anil, and salicylaldehyde anil derivatives.

125- $\mu\text{m}$  radius for the spherical iron beads. Thus, our charge densities are 5–10 times higher, which is not surprising given the different experimental designs in the two studies. Unlike our powder/bead rolling procedure, in Gibson's experiment<sup>13</sup> the charge was developed by rolling the beads down and inclined film of the aromatic anil derivatives and collecting them in a Faraday cage. A critical difference between the experimental designs is the contact times. In our experiments, the charge is equilibrated at 3 min, although we have no information on the very initial charge levels. In Gibson's experiments, the short contact times (less than 1 s) resulting from rolling beads down the 9-in. plane inclined at 30° may only give initial charge levels even though variations of this design are reported to gave an equilibrated charge.<sup>24,25</sup> Even if equilibrium charge is attained, the limited surface area provided by the film-coated surface may limit the charge levels. This consideration alone can account for the charge differences between our results and Gibson's results, even though many factors are known to influence the charge.<sup>26–29</sup> It should be noted that charge variations of 1 order of magnitude or more are often observed in the studies with organic materials.<sup>23</sup>

If the charge results from electron transfer, the molecules in the solid must oxidize as shown in eq 1, and a direct



relationship is expected between the charge and the half-wave oxidation potentials ( $E_{1/2}$ ) for the compounds as pointed out by Cressman.<sup>12</sup> This relationship should exist even though the comparison is between solid state

(24) Waelin A.; Baekstroem, G. *J. Appl. Phys.* 1974, 45, 2058.

(25) Cottrell, G. A. *J. Phys. D: Appl. Phys.* 1978, 11, 681.

(26) Lowell, J. *J. Phys. D, Appl. Phys.* 1976, 9, 1571.

(27) Lowell, J. *J. Electrostat.* 1987, 20, 233.

(28) Homewood, K. P.; Rose-Innes, A. C. *Static Electrification*; Inst. Phys. Conf. Ser., 1979; No. 48, 233.

(29) Akande, A. R.; Lowell, J. *J. Phys. D, Appl. Phys.* 1987, 20, 565.

(22) Surface area value from BET analysis: Moore, M. IBM Boulder Co., private communication.

(23) Lowell, J.; Rose-Innes, A. C. *Adv. Phys.* 1980, 29, 947.

and liquid solution. The difference between the lattice interactions and the solvation should manifest itself in the slope. This is certainly the case for linear correlations between gas-phase ionization potentials and solution  $\sigma$  parameters,<sup>30</sup>  $E_{1/2}$ ,<sup>31</sup> and bromination rates.<sup>32</sup> We measured the oxidation potentials of the various derivatives and found agreement with the literature values.<sup>33-35</sup> The values are listed in Table I and are plotted against  $\log(Q/N)$  in Figure 2.  $\log(Q/N)$  values for aniline and for *p*-nitroaniline are absent from the plot because the former is a liquid and was not included in the charging experiments and the latter charges negative.  $\log(Q/N)$  varies linearly with  $E_{1/2}$  for both the aniline derivatives ( $R = 0.99$ ) and the two aromatic aldehyde anil derivatives ( $R = 0.97$ ) as expected; however, each derivative series forms a separate line. The slopes are close,  $-3.6$  and  $-3.4$  for the two series, indicating sensitivities to the electronic effects of the substituents. Thus, there is a parallel response in the energetics for the charging and the oxidation reactions (eqs 1 and 2); however, a single line is expected if charging is a simple electron-transfer process. The aniline derivatives charge lower than the aldehyde anils (except  $Q/N$  of AN-NH<sub>2</sub>) even though they are more easily oxidized (lower  $E_{1/2}$  values). Furthermore, *p*-nitroaniline charges negative while the other derivatives charge positive. As mentioned in the Introduction, a change in sign requires the energy of the HOMO level to shift by ca. 3.4 eV, which is the HOMO-LUMO energy difference of aniline molecules (from UV data). However, the range in the oxidation potentials from the *p*-methylaniline (charges positive) and *p*-nitroaniline (charges negative) indicates less than 0.6-eV difference between the HOMO levels of these compounds. Therefore, it is unlikely that electron transfer occurs between the iron beads and the organic compounds, even though electrons can transfer when the HOMO and LUMO levels of the organic materials and the Fermi level of the metal are not energetically matched.

Given the existence of the  $\log(Q/N) - \sigma$  linear relationship, it is not surprising to find  $\log(Q/N)$  also linear with  $pK_b$ , which reflects the basicity of the compounds, because linear  $pK_b - \sigma$  relationships are well-known for many derivative series including the aniline derivatives. The  $\log(Q/N)$  vs  $pK_b$  plot is shown in Figure 3 for some aniline derivatives. The  $pK_b$  values (7.84 for NH<sub>2</sub>, 8.66 for OCH<sub>3</sub>, 8.90 for CH<sub>3</sub>) were obtained by subtracting the literature  $pK_a$  values<sup>36</sup> from 14. This linear relationship ( $R = 0.96$ ) suggests that the contact charge could be a result of proton transfer. Unfortunately, the  $pK_b$  values for the salicylaldehyde and benzaldehyde anil compounds are not available since these compounds are hydrolytically unstable to the measurement conditions.<sup>37</sup> The fact that the charge correlates well with both  $\sigma$  and  $pK_b$  demonstrates the weakness of using linear free energy relationships alone for concluding the mechanism of charging.<sup>12,13</sup>

The metal beads were recovered after the rolling and blowoff step to determine the amount of material transfer

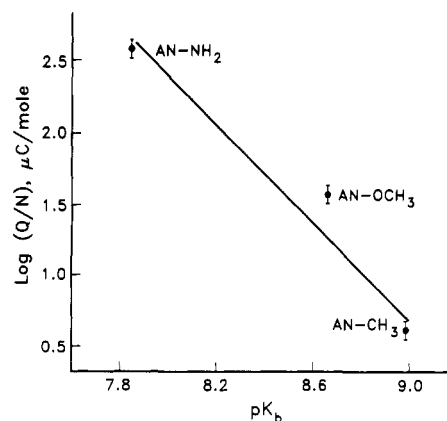


Figure 3. Plot of  $\log(Q/N)$  against  $pK_b$  for the substituted aniline derivatives.

accompanying the charge transfer. The determination was made spectroscopically so it is the intact aromatic aldehyde anil being measured. As seen in Table II the amount of material found on the beads ( $N_R$ ) is considerable and is in the range 0.4–2.3  $\mu\text{mol/g}$  of bead. The same amount of material (within 10%) was found on the beads after 3 and 30 min total rolling time. Therefore, there appears to be an “end point” to the amount of material that will adhere to the beads. Inspection of the beads by SEM after removal of the powder by blowoff does not reveal the presence of any large amounts of powder (Figure 4). Again using the specific surface area for the beads (400  $\text{cm}^2/\text{g}$ ) provides a surface density range of  $(1-6) \times 10^{-9}$   $\text{mol}/\text{cm}^2$ , or  $(6-36) \times 10^{14}$   $\text{molecules}/\text{cm}^2$ . Thus it appears that the accumulation of material on the surface of the beads stops soon after 1–9 monolayers are deposited. The complication of material transfer was never mentioned in the reports by Cressman<sup>12</sup> and Gibson.<sup>13</sup> It clearly points to the inadequacy of using molecular solids or in some cases even polymers<sup>38</sup> for contact charging. Although some transfer is inevitable, we find it to be minimal when using a high molecular weight, tougher, styrenic polymer.<sup>17</sup>

There is a linear log-log relationship ( $R = 0.97$ ) between the charge and the amount of material on the bead (Figure 5). *p*-Nitroaniline was not included because it charges negative. The slope of this linear free energy relationship between the two processes (eqs 1 and 3) implies that the charge-transfer process is 3 times more sensitive to structural changes than the material transfer process. It also anticipates the linear correlation between the amount of organic material on the metal beads and the base strength of the compounds. The two processes can be viewed in terms of Lewis acid/base chemistry where the aniline and the aromatic anil derivatives are the bases and the proton and the metal surface are the acids. During contact and separation, the exchange processes that occur are the transfer of an aromatic molecule from the surface of the powder to the surface of the metal beads (eq 3), and proton transfer to a basic site on the surface of the powder from the dissociation of surface OH groups or moisture on the beads (eq 4). Surface OH groups are considered here because XPS analysis of the beads indicates the presence of an oxide layer, which comes as no surprise. The presence of moisture (humidity) has certainly been reported to affect the charging.<sup>39,40</sup> While we did not control the

(30) Buchs, A. *Helv. Chim. Acta* 1970, 53, 2026.

(31) Dibble, T.; Bandyopadhyay, S.; et al. *J. Phys. Chem.* 1986, 90, 5275.

(32) McAlduff, E. J.; Chan, T. *Can. J. Chem.* 1978, 56, 2714.

(33) Kudez, J. E.; Gibson, H. W.; Wychick, D. *J. Org. Chem.* 1975, 40, 875.

(34) Siegerman, H. In *Techniques of Electroorganic Synthesis*, Part II; Weinberg, N. L., Ed.; Wiley: New York, 1975.

(35) Nelson, R. F. In *Techniques of Electroorganic Synthesis*, Part I; Weinberg, N. L., Ed.; Wiley: New York, 1974.

(36) Smith, J. W. In *The chemistry of the amino group*; Patai, S., Ed.; Wiley: London, 1968.

(37) Smith, J. W. In *The chemistry of the carbon-nitrogen double bond*; Patai, S., Ed.; Wiley: London, 1970.

(38) Salaneck, W. R.; Paton, A.; Clark, D. T. *J. Appl. Phys.* 1976, 47, 144.

(39) Folan, L. M.; Arnold, S.; O'Keeffe, T. R.; Spock, D. E.; Schein, L. B.; Diaz, A. F. *J. Electrostat.* 1990, 25, 155.

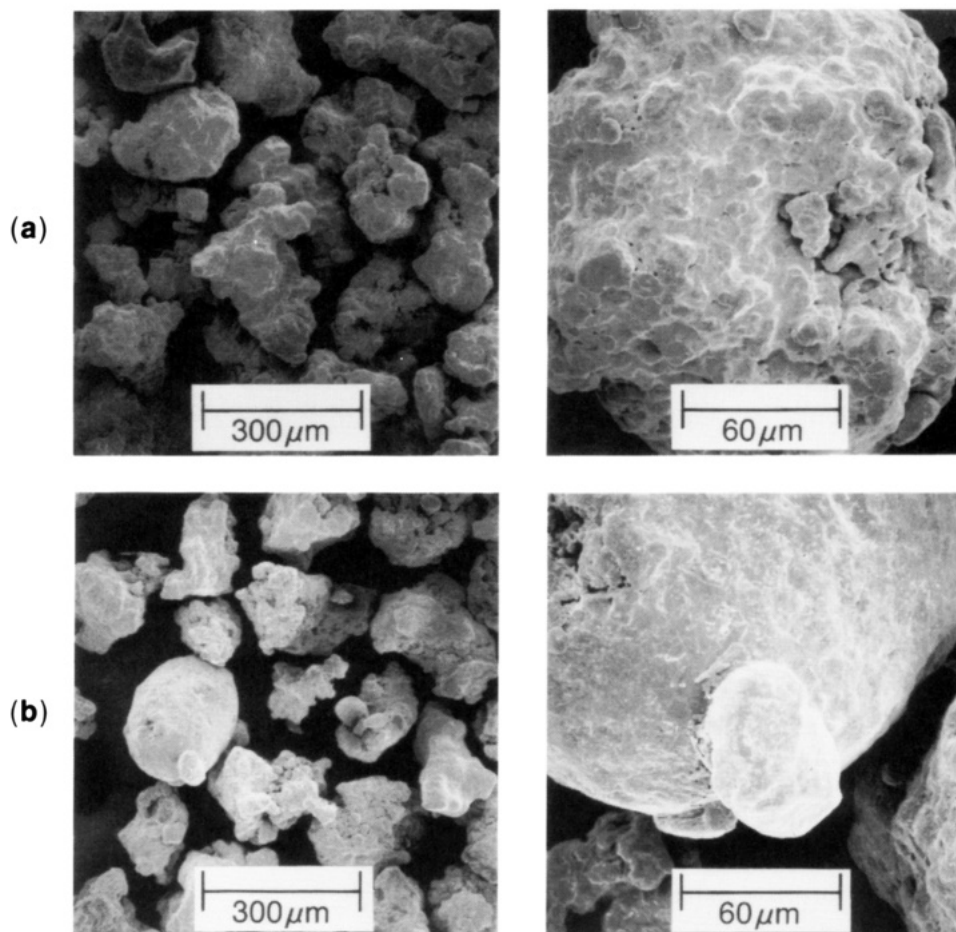


Figure 4. Scanning electron micrographs of iron beads (a) before contact and (b) after recovery from contact and blowoff of the powder.

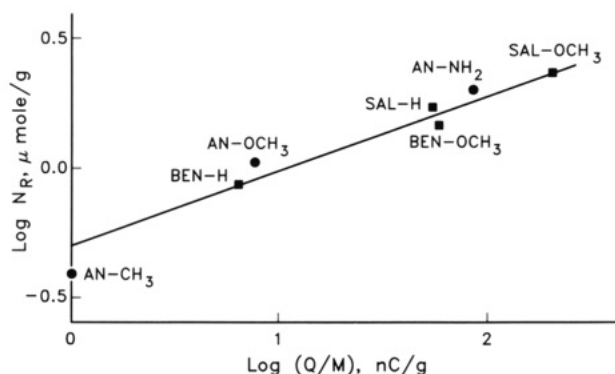


Figure 5. Plot  $\log N_R$  against  $\log (Q/M)$  for the various substituted derivatives.

humidity, the ambient conditions were fairly constant with the temperature at 68–70 °F and the relative humidity at 49–53% for all the measurements. Humidity changes do not affect the charging trend within a series, however, because we reproduce Gibson's trend and his measurements were made at 0% humidity.<sup>13</sup>

#### Summary: Electron vs Ion Transfer

In the early 1950s, Harper<sup>14</sup> proposed an electron-transfer mechanism to explain contact charging between metals. Harper's results<sup>14</sup> showed that the charge transfer is proportional to the contact potential difference ( $V_c$ ) of the metals which is defined by  $V_c = (\phi_b - \phi_a)/e$ , where  $\phi_a$  and  $\phi_b$  are the work function of the metals and  $e$  the

electron's charge. Some years later, electron transfer was extended to explain the charge between metals and insulators because like the metal-metal case, the charge on the polymer was found to depend on the contact potential difference.<sup>23,41,42</sup> Unfortunately, the scatter in the charge-transfer data often makes it difficult to determine the exact relationship between the charge and the work function of the contacting metal. A qualitative relationship between the charge and the electronic effects of the substituents on the compounds (Hammett  $\sigma$ ) was established by Cressman et al.<sup>12</sup> and Gibson<sup>13</sup> and was used as support for the electron-transfer mechanism.<sup>23</sup> Unfortunately, a Hammett  $\sigma$  relationships is not a proof of the existence of electron transfer. It does not even permit a distinction between electron and ion transfer because both processes will relate linearly with Hammett's  $\sigma$ . This is because the electronic effects of the substituents affect both the electronic and the chemical properties (like acidity/basicity, redox) of the molecules. The change in sign of the charge within a series of substituted derivatives is difficult to accommodate with the electron-transfer mechanism because the amount of energy required to detach an electron makes gross demands on the relative positions of the donor-acceptor levels. A further complication not yet mentioned arises from the presence of surface oxide layers on metals and carbon.<sup>43</sup> The charging can often be a surface process<sup>44,45</sup> which correspondingly varies with the

(41) Davies, D. K. Br. J. Appl. Phys.: J. Phys. D 1969, 2, Ser. 2, 1533.

(42) Davies, D. K. Static Electrification; Inst. Phys. Conf. Ser., 1967; No. 4, p 29.

(43) Fabish, T. J.; Hair, M. L. J. Colloid Interface Sci. 1977, 62, 16.

(44) Hays, D. A. Static Electrification; Inst. Phys. Conf. Ser., 1979, No. 48, p 265.

(40) Matsui, M.; Oka, K.; Inaba, U., The 6th International Congress on Advances in Non-Impact Printing Technologies, 1990; p 45.



surface composition and not necessarily respond to the Fermi levels.

In conclusion, a relationship with the Hammett  $\sigma$  is not a proof of electron transfer. For the present case the results are better explained in terms of ion transfer, most likely proton transfer. This mechanism is particularly favored considering the amount of energy required to detach electrons in ambient conditions. The change in the sign of the charge within a series can in principle result from a change in the direction of proton transfer when there is a shift in the relative basicities of two closely matched materials. This sign change is difficult to explain in terms of changes in the relative donor/acceptor energy levels. Thus, there is no need to invoke the electron-

transfer mechanism, even though it cannot be ruled out. In concurrence with Kornfield,<sup>8</sup> we believe that ions transfer between two surfaces, and the direction and amount of transfer will depend on the relative basicity and "ion affinities" of the surfaces. Finally, we find that these aniline and anil derivatives are not appropriate for studying charging mechanisms because of the large amount of material transfer between the two surfaces.

**Acknowledgment.** We thank Jose Vazquez and David Dreblow for their technical assistance with certain aspects of this study. J.G. is grateful to the Natural Sciences and Engineering Research Council of Canada for a postdoctoral fellowship.

**Registry No.** SAL-H, 779-84-0; SAL-OCH<sub>3</sub>, 889-08-7; BEN-OCH<sub>3</sub>, 783-08-4; BEN-H, 538-51-2; AN-NO<sub>2</sub>, 100-01-6; AN-CH<sub>3</sub>, 106-49-0; AN-OCH<sub>3</sub>, 104-94-9; AN-NH<sub>2</sub>, 106-50-3; Fe, 7439-89-6.

(45) Homewood, K. P. *J. Phys. D: Appl. Phys.* 1984, 17, 1255.

## Characterization of Copper(II)-Substituted Synthetic Fluorohectorite Clay and Interaction with Adsorbates by Electron Spin Resonance, Electron Spin Echo Modulation, and Infrared Spectroscopies

Vittorio Luca, Xinhua Chen, and Larry Kevan\*

*Department of Chemistry, University of Houston, Houston, Texas 77204-5641*

*Received May 24, 1991. Revised Manuscript Received September 16, 1991*

Fluorohectorite containing lattice Cu(II) is synthesized and characterized by electron spin resonance (ESR) and electron spin echo modulation (ESEM) spectroscopies. Three Cu(II) species are identified in the ESR spectrum of this Cu(II)-substituted fluorohectorite. Species A and B have hyperfine splitting constants of  $118 \times 10^{-4}$  and  $50 \times 10^{-4} \text{ cm}^{-1}$ , respectively, while species C gives spectra that are not well resolved from the  $g_{\perp}$  region of species A and B. On the basis of ESEM measurements, species B is assigned to Cu(II) in octahedral sites with Li(I) in a neighboring octahedral site and species A is assigned to Cu(II) in octahedral sites with no Li(I) in a neighboring octahedral site. Species C is assigned to coordinatively unsaturated Cu(II) sites that are part of the octahedral sheet but that are at the termination of the crystallites, i.e., edge lattice sites. At activation temperatures of 400 °C, species C sites interact strongly with Lewis bases such as pyridine and ammonia. Infrared measurements show that species C sites have moderate Lewis acid strength and also apparently coordinate water molecules but not benzene.

### Introduction

The strength of interaction between an adsorbate molecule possessing functional groups such as O or N and metal ions imbedded in a host lattice depends on the electron-donating capability of the adsorbate molecule and the electron-accepting capability of the metal ion (Lewis acid). The transition metals with partially occupied d orbitals possess relatively strong coordinating properties (i.e., they are strong Lewis acids). It is the Lewis acid strength of the transition-metal ions which controls their catalytic activity. The Lewis acid strength depends not only on the nature of the metal ion but also on the interaction of the metal with the substrate.

Clay minerals possess a melange of surface-active sites.<sup>1</sup> Here we focus on transition-metal-ion sites in smectite clays. These can be divided into ion-exchange sites in the interlayer space and lattice sites within the clay structure.

In smectite clays there are both octahedrally and tetrahedrally coordinated sites in the clay layer. In nature, smectite clay minerals are found that contain a variety of transition-metal ions in lattice sites. For instance Cr(III), V(III), Ti(III), and Mn(II) are found substituting to various extents in octahedral sites for the more common lattice ions such as Si(IV), Al(III), Fe(III), Fe(II), and Mg(II).<sup>2-4</sup>

Laszlo and Mathy<sup>5</sup> have shown the potential for organic synthesis by natural clay minerals with transition-metal ions in exchange sites. Fewer studies have dealt with the effects of transition-metal ions in lattice sites. Wheeler and Thomas<sup>6</sup> provided evidence that Cu(II) cations in lattice sites in synthesized hectorite have a marked effect on the photochemistry of adsorbed [4-(1-pyrenyl)butyl]-trimethylammonium cation. Ni-substituted synthetic mica-montmorillonite clays have also been shown to be

(1) Coyne, L. M. In *Spectroscopic Characterization of Minerals and their Surfaces*, Coyne, L. M., McKeever, S. W. S., Blake, D. F., Eds.; ACS Symposium Series 415; American Chemical Society: Washington, D.C., 1990; Chapter 1.

(2) McCormack, G. R. *Clays Clay Miner.* 1978, 26, 93.

(3) Gerald, P.; Herbillon, A. J. *Clays Clay Miner.* 1983, 31, 143.

(4) Foord, E. E.; Starkey, H. C.; Taggart, J. E.; Shawe, D. R. *Clays Clay Miner.* 1987, 35, 139.

(5) Laszlo, P.; Mathy, A. *Helv. Chim. Acta* 1987, 70, 577.

(6) Wheeler, J.; Thomas, J. K. *Langmuir* 1988, 4, 543.